



November 1966

Third Quarterly Report

Covering the Period 1 January to 31 July 1966

STUDY AND APPLICATIONS OF RETRODIRECTIVE AND SELF-ADAPTIVE ELECTROMAGNETIC WAVE CONTROLS TO A MARS PROBE

Prepared for:

NATIONAL AERONAUTICS AND SPACE ADMINISTRATION
TECHNICAL INFORMATION DIVISION
AMES RESEARCH CENTER
MOFFETT FIELD, CALIFORNIA

CONTRACT NAS 2-2933

By: C. A. HACKING C. H. DAWSON

SRI Project 5574

Approved: R. C. HONEY, MANAGER
ELECTROMAGNETIC TECHNIQUES LABORATORY

D. R. SCHEUCH, EXECUTIVE DIRECTOR
ELECTRONICS AND RADIO SCIENCES

Copy No. **3**

ABSTRACT

This report primarily concerns the effects on the spectrum of a received or transmitted CW signal associated with one or the other of two antennas each having a generally cylindrical configuration and spinning about its axis.

The spectrum associated with a single element on such an antenna is very broad, with high energy content in high-order sidebands. However, the effect of spinning, on the retransmitted spectrum, of a complete retrodirective antenna is shown to be quite small.

CONTENTS

ABSTRACT	ii
LIST OF ILLUSTRATIONS.	iv
LIST OF TABLES	v
I INTRODUCTION.	1
II SPECTRAL SPLITTING	3
A. Type-3 Antenna.	3
B. Type-1 Antenna.	5
1. One-Way-Transmission Case	5
2. Considerations of Total Spectral Power.	12
3. The Retrodirective-Array Case	13
a. Gain in the Retrodirective Direction.	13
b. Spectral-Power Content.	16
III ANALYSIS.	19
A. Spectral Splitting at a Single Element.	19
1. Type-3 Antenna.	19
2. Type-1 Antenna.	20
3. Spectral Splitting in an Adaptive Receiving Antenna	21
B. Spectral Splitting and Retrodirective Arrays.	21
APPENDIX A SPECTRAL SPLITTING FOR A SINGLE ELEMENT IN A CIRCULAR ARRAY OF OMNIDIRECTIONAL ELEMENTS (TYPE-3 ANTENNA).	23
APPENDIX B DERIVATION OF SPECTRUM IN THE CYLINDRICAL-GEODESIC-LENS BICONICAL-HORN ADAPTIVE (TYPE-1) ANTENNA DUE TO VEHICLE ROTATION.	29
APPENDIX C DERIVATION OF POWER IN THE TYPE-1 ANTENNA.	36
APPENDIX D RETRANSMITTED SIGNAL FROM A CYLINDRICAL-GEODESIC-LENS BICONICAL-HORN ADAPTIVE (TYPE-1) ANTENNA	40
REFERENCES	45

ILLUSTRATIONS

Fig. 1	Omniazimuth-Element Circular Array on the End of a Cylinder (Type-3 Antenna)	4
Fig. 2	Relative Energy Content of Each Sideband for a Single Elemental Radiator Moving on the Circumference of a Circle	5
Fig. 3	Cylindrical-Geodesic-Lens Biconical-Horn Adaptive Antenna (Type-1 Antenna)	6
Fig. 4	Ray Geometry Associated with a Single Radiator and Single Azimuth	7
Fig. 5	Cumulative Power for a Single Element <i>vs.</i> Sideband Number.	8
Fig. 6	Ray 0—Relative Power in dB for Each Spectral Line	10
Fig. 7	Rays -1, +1—Relative Power in dB for Each Spectral Line	11
Fig. 8	Rays -1, 0, +1—Relative Power in dB for Each Spectral Line.	12
Fig. 9	Retrodirective Gain as a Function of Azimuthal Position.	14
Fig. A-1	Geometry of Phase Centers of Elemental Omnidirectional Radiators	24

TABLES

Table I	Gain and Sideband Power for a 60-Element, Cylindrical-Geodesic-Lens Biconical-Horn (Type-1) Antenna in the Retrodirective Mode	17
Table A-1	Spectral Content vs. Sideband Number.	27

I INTRODUCTION

This is the Third Quarterly Report of a study to investigate some of the many possible uses of adaptive antenna circuits for communication to and between vehicles on an interplanetary mission. It is assumed that the main vehicle, the *bus*, flies by or orbits the target planet and when in the vicinity releases a smaller vehicle, the *capsule*, to enter the planet's environment for a hard or soft landing. Communication between the earth and the bus is specified as being within the presently used S-band of frequencies, but between the bus and capsule the best frequency of operation is presently a subject of study. In addition to communication, the adaptive antenna circuitry should be considered for other purposes as well, such as providing navigational and environmental information.

One of the arbitrary ground rules applied to this study so far is to assume that the vehicles will be spin-stabilized, particularly the bus. Consequently, provided the spin axis is correctly chosen, all active stabilization is eliminated except for that due to minor perturbations like solar wind, etc. It also means that only one-dimensional "scanning" of the retrodirective or self-adaptive reviewing antenna is needed, thus leading to a higher antenna gain for a given number of elemental radiators, but this one dimension must obviously scan continuously through 360 degrees.

In the two previous quarterly reports, four different cylindrical antenna configurations were investigated analytically. The primary concern was to make comparisons between the antenna gain to be expected from the several configurations. Some problems were encountered in computing the gain, but much of this was related to the various definitions of gain that can be used. These are not always consistent.

The First Quarterly Report included a study of the conditions to be expected in the vicinity of Mars, particularly as they would relate to communications with a capsule entering Martian environment. Also, in the First Quarterly Report the analysis was started of a particular cylindrical antenna configuration in which all the receiver/transmitter elements are used for any azimuthal direction of the antenna beam. This was done by

focusing the energy to and from the elemental radiators by means of a cylindrical geodesic lens. For this antenna the computed gain was generally less than one dB below the postulated theoretical maximum value and required no switching of elements as the vehicle rotated.

These original computations were greatly simplified by assuming that the retransmitted signal had exactly the same frequency as the incoming pilot signal. This work has now been extended, and its accuracy has been increased, particularly to study some aspects of spectral splitting associated with an antenna of this type. The more realistic case of different transmit and receive (pilot) frequencies has been considered.

The report is confined to some of these aspects of spectral splitting of a spinning antenna.

II SPECTRAL SPLITTING

When an antenna is spinning about an axis not in the plane of the received or transmitted signal, the spinning results in periodic frequency modulation (and possibly amplitude modulation) of the signal. This effect is called *spectral splitting*.

A. Type-3 Antenna

The first situation considered is for a single element in a circular array of theoretically omnidirectional elements as shown in Fig. 1. Various other aspects of this and similar antennas have been discussed elsewhere.^{1*} The antenna is assumed to be either only receiving or only transmitting a CW signal. The result is a spectrum having lines at the CW frequency and at lower and higher frequencies separated from the CW frequencies by multiples of the spin frequency. The spectrum peaks in the neighborhood of $2\pi Rf_s$, where

R = Distance of the element from the spin axis
(radius) in wavelengths

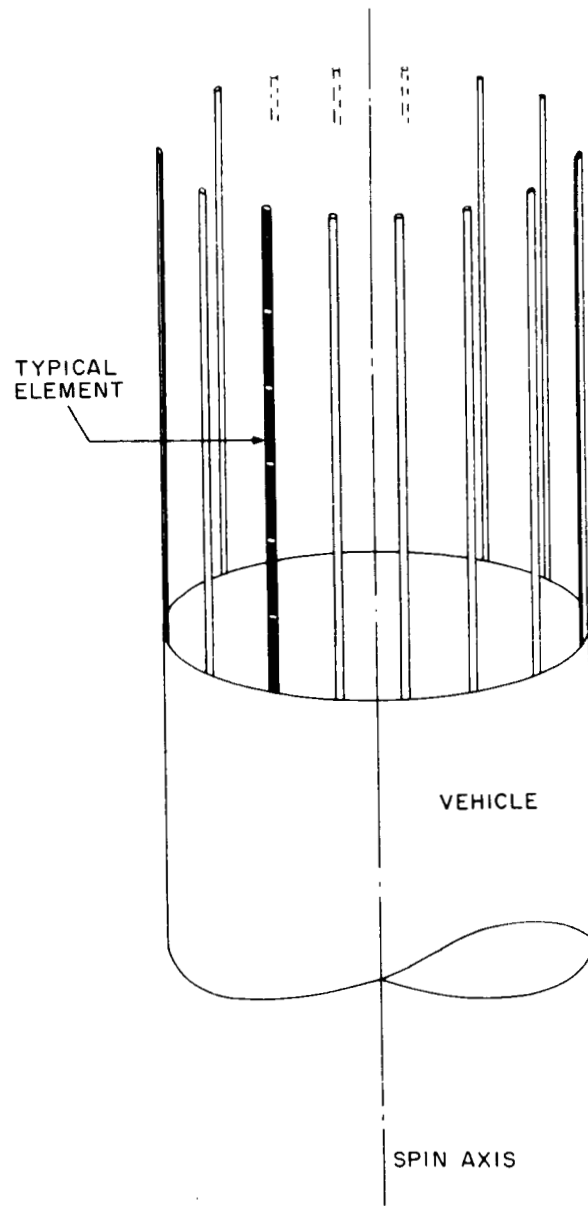
f_s = Spin frequency.

The spectrum is derived in Appendix A, and the values associated with a particular antenna configuration are tabulated there. A plot of the relative power in each of the upper sidebands is shown in Fig. 2. The complete power spectrum is symmetrical about the carrier frequency f_0 (sideband number = 0).

It can be seen that the *maximum* power occurs in the sixtieth sideband, but it is insignificant for all sideband numbers greater than 70. Since only one elemental radiator has been considered, these numbers cannot be associated with the number of elements; they are in fact related to the path length of the element for one spin revolution ($2\pi R$).

It will be noted that this length is 63.61 wavelengths for the model represented in Fig. 2.

* References are listed at the end of the report.



TA-5574-33

FIG. 1 OMNIAZIMUTH-ELEMENT CIRCULAR ARRAY ON THE END OF A CYLINDER (Type-3 Antenna)

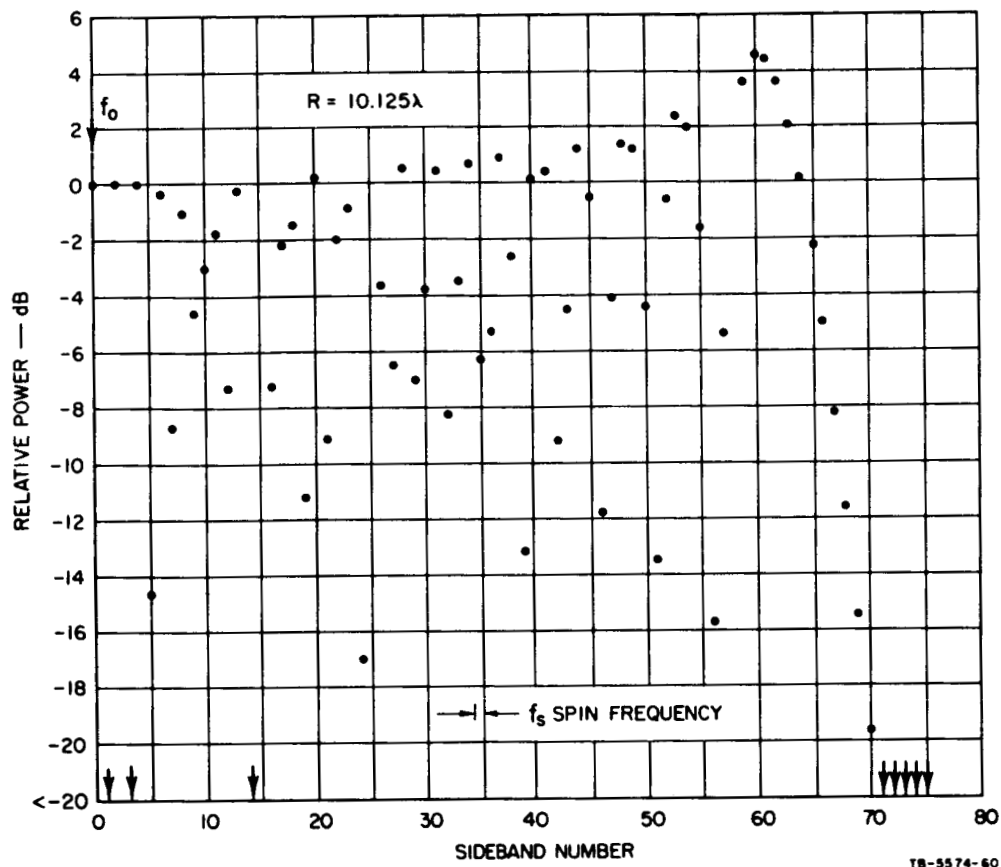


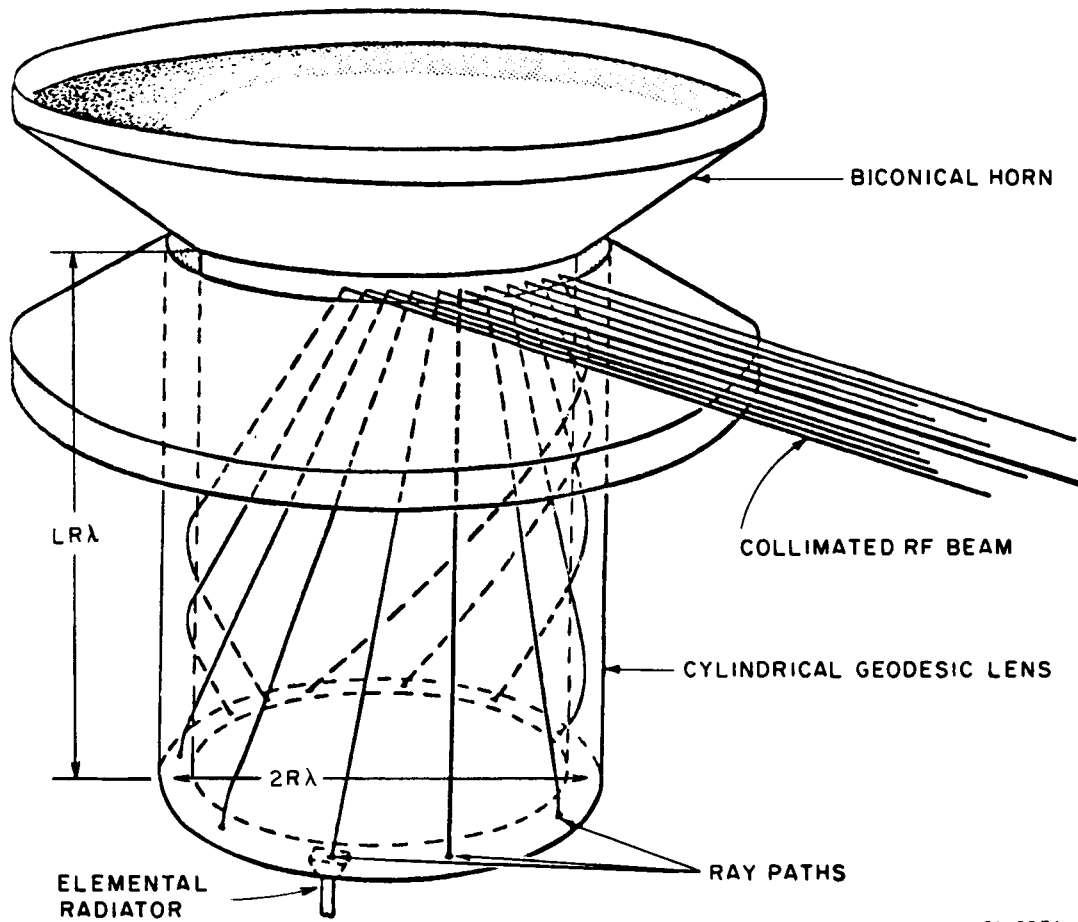
FIG. 2 RELATIVE ENERGY CONTENT OF EACH SIDE BAND FOR A SINGLE ELEMENTAL RADIATOR MOVING ON THE CIRCUMFERENCE OF A CIRCLE

B. Type-1 Antenna

The remaining work on spectral splitting concerns the cylindrical-geodesic-lens biconical-horn adaptive antenna as shown in Fig. 3.

1. One-Way-Transmission Case

First a single element operating only in either the receive or transmit mode was studied, as explained in Appendix B. The method used allowed the spectrum of the individual rays to be determined. The ray geometry is basically the same as that used in previous computations² and is shown in Fig. 4.



TA-5574-1

FIG. 3 CYLINDRICAL-GEODESIC-LENS BICONICAL-HORN ADAPTIVE ANTENNA
(Type-1 Antenna)

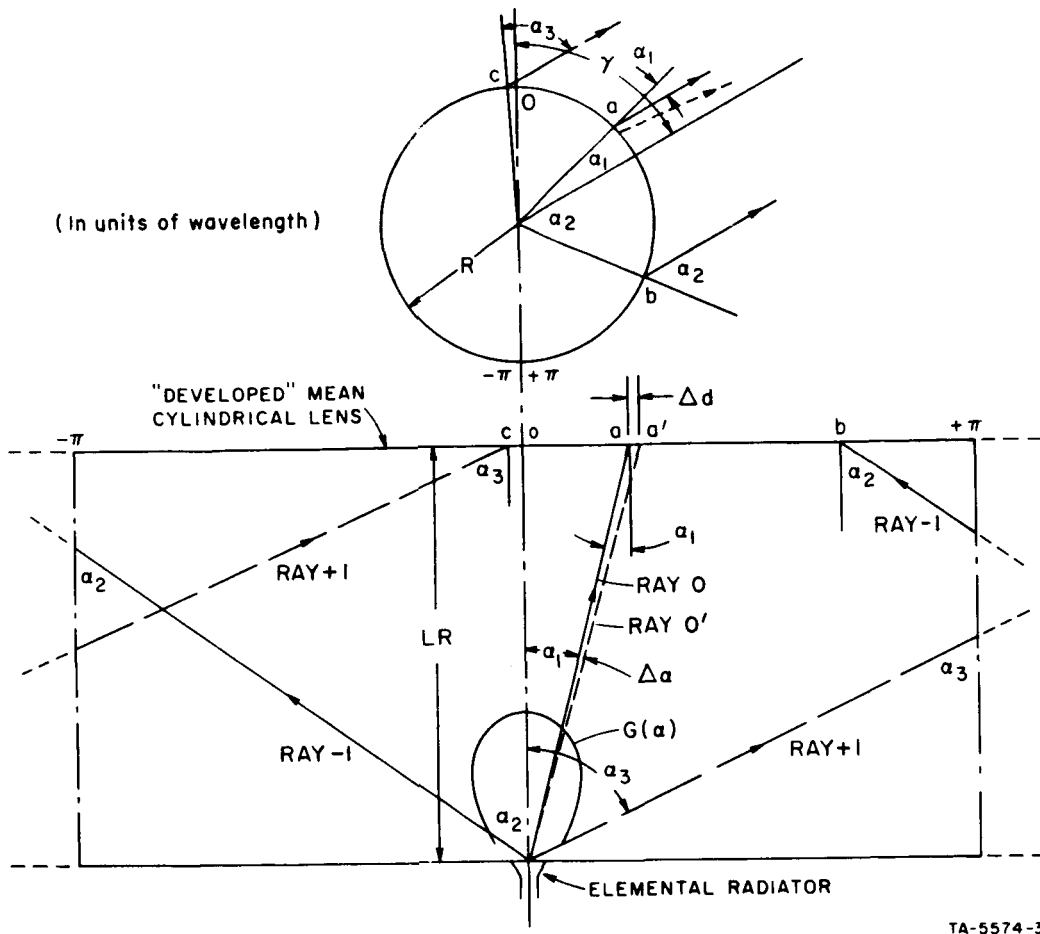


FIG. 4 RAY GEOMETRY ASSOCIATED WITH A SINGLE RADIATOR AND SINGLE AZIMUTH ANGLE

Various computations were made for an antenna model having a cylindrical lens radius, R , of 10λ , and axial length-to-radius ratio, L , of 3.0 and a particular elemental gain function $G(\alpha)$.

Only the three most significant rays associated with a particular antenna element and a particular azimuthal direction were considered; they are referred to as Rays 0, +1, and -1. (In the original study of this Type-1 antenna² only two such rays were considered; they were referred to as Ray 1 and Ray 2).

The computation techniques used allow the separation of several combinations of rays, and they are presented in the data in the following groupings:

- Ray 0
- Rays -1 and +1
- Rays -1, 0, and +1 .

Higher-order rays, which must travel at least one helical revolution within the cylindrical geodesic lens contribute negligible power for the particular values of the parameters used in these calculations. In this particular antenna configuration the cylindrical lens has a radius of 10 wavelengths and the elemental radiator has an aperture of one-sixtieth the circumference of the lens [which determines what the value of $G(\alpha)$ will be].

Figure 5 is a curve of cumulative power (on a linear arbitrary scale) vs. sideband number for these three combinations.

Note that practically all the power of Ray 0 falls in Sidebands 0 to 40 while that of Rays -1 and +1 falls in Sidebands 40 to 60. This relates to the time rate of change of phase which is proportional to $\sin \alpha$. Since

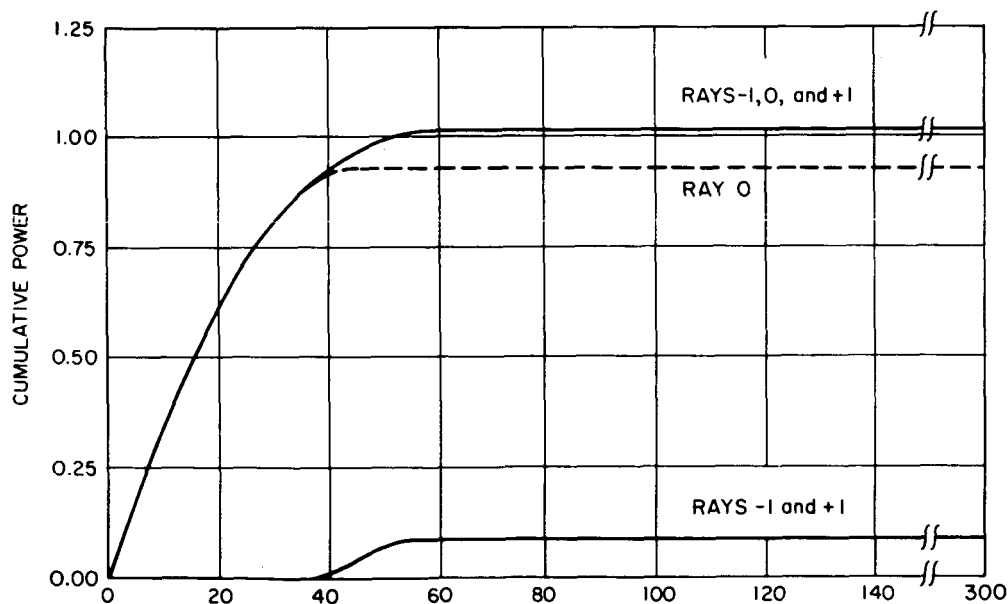


FIG. 5 CUMULATIVE POWER FOR A SINGLE ELEMENT vs. SIDEBAND NUMBER

the ranges of α are discontinuous (or disjoint) for Ray 0 and Rays -1 and +1, it is not surprising that their spectra are disjoint (*i.e.*, complement each other, as seen from Figs. 6 and 7).

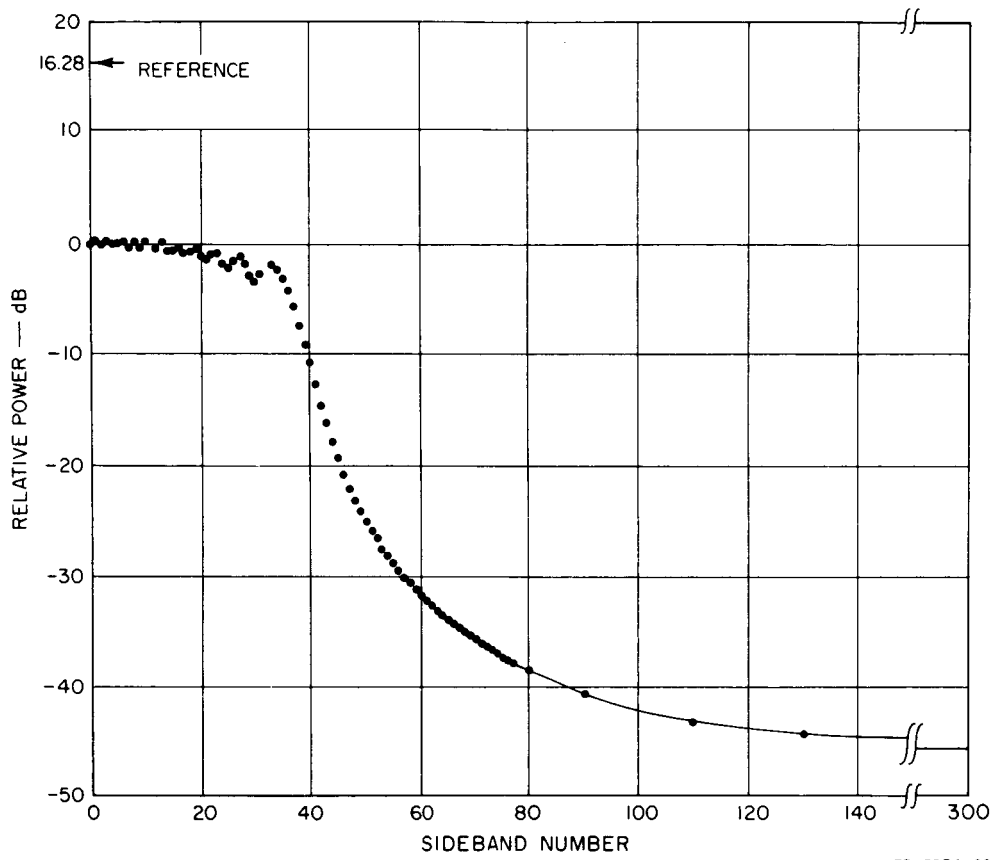
Figures 6, 7, and 8 present the spectra for Ray 0, Rays -1 and +1, and Rays -1, 0, and +1 respectively. The spectra for larger sideband numbers were also calculated but have not been plotted since they are essentially random and since Fig. 5 shows their minimal contribution to the total power. The level labelled "reference" in Figs. 6, 7, and 8 corresponds to the maximum cumulative power shown in Fig. 5.

Again the spectrum for Ray 0 is disjoint with that for Rays -1 and +1 and the latter pair alone gives rise to the irregular behavior above Sideband 60.

Since the integrations called for in Eqs. (B-26) and (B-27) of Appendix B are actually computed as sums over a finite set of points, our confidence in the results goes down as the sideband number goes up because the number of samples per cycle of the harmonic goes down. The accuracy obtained is, however, more than adequate for the present study.

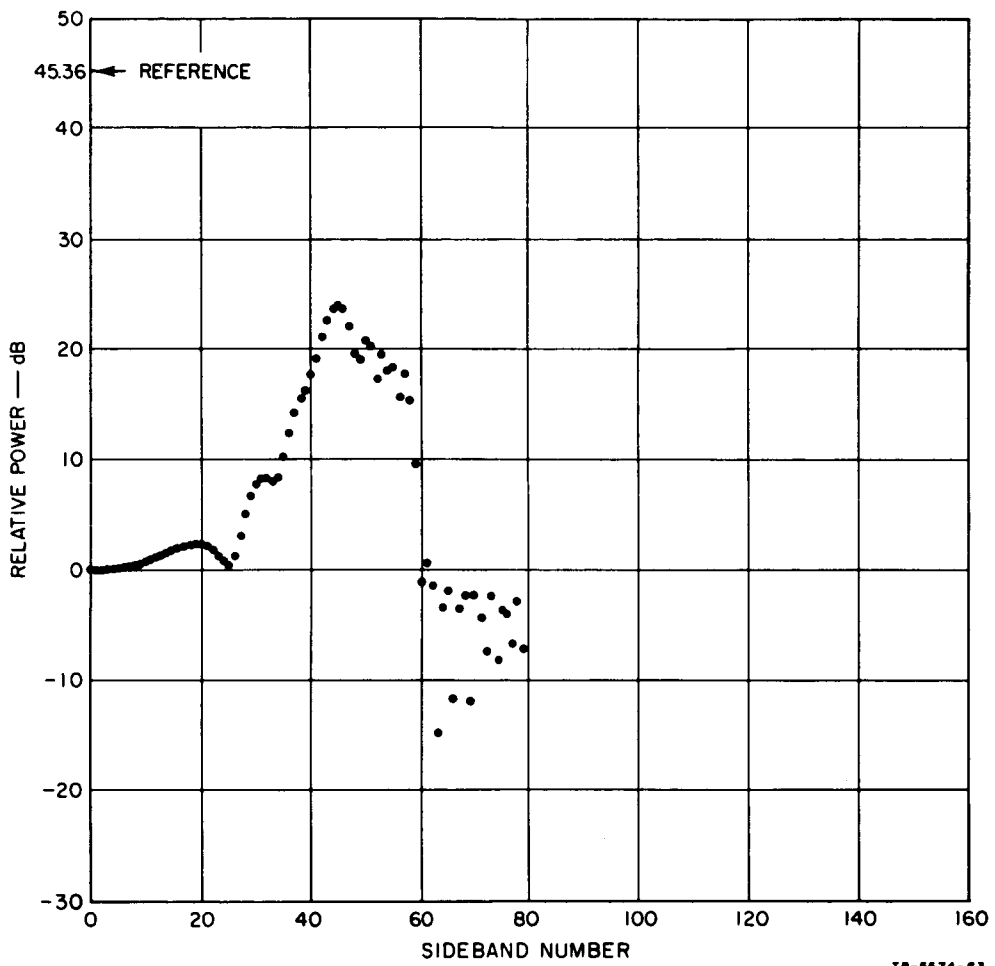
It can therefore be concluded that there is spectral splitting in this type of antenna, with appreciable power out to about the 60th sideband, which might be a serious drawback for certain types of array. However, the resulting spectrum does peak at the carrier frequency in contrast to the configuration considered earlier (see Fig. 2) where the spectrum peaked at about the 60th sideband. This can be attributed to the fact that in this Type-1 antenna, when the element is moving with highest radial velocity—that is, at the limbs of the complete cylindrical antenna—it has relatively low gain in the direction of interest. However, in the Type-3 antenna, the elemental gain is theoretically constant at all values of radial velocity.

If all the elemental radiators of the antenna are active phase-conjugated re-radiators and are identical, to an observer at a fixed point the antenna must look the same after a rotation of $2\pi/N$ radians, where N is the number of elemental radiators. Thus when the antenna is considered as a whole, the spectrum can contain only sidebands whose numbers are multiples of N . Of course, if the elements are not identical or if one or more is otherwise faulty, the intermediate sidebands will not disappear. The spectral contribution from each faulty element will, however, be small



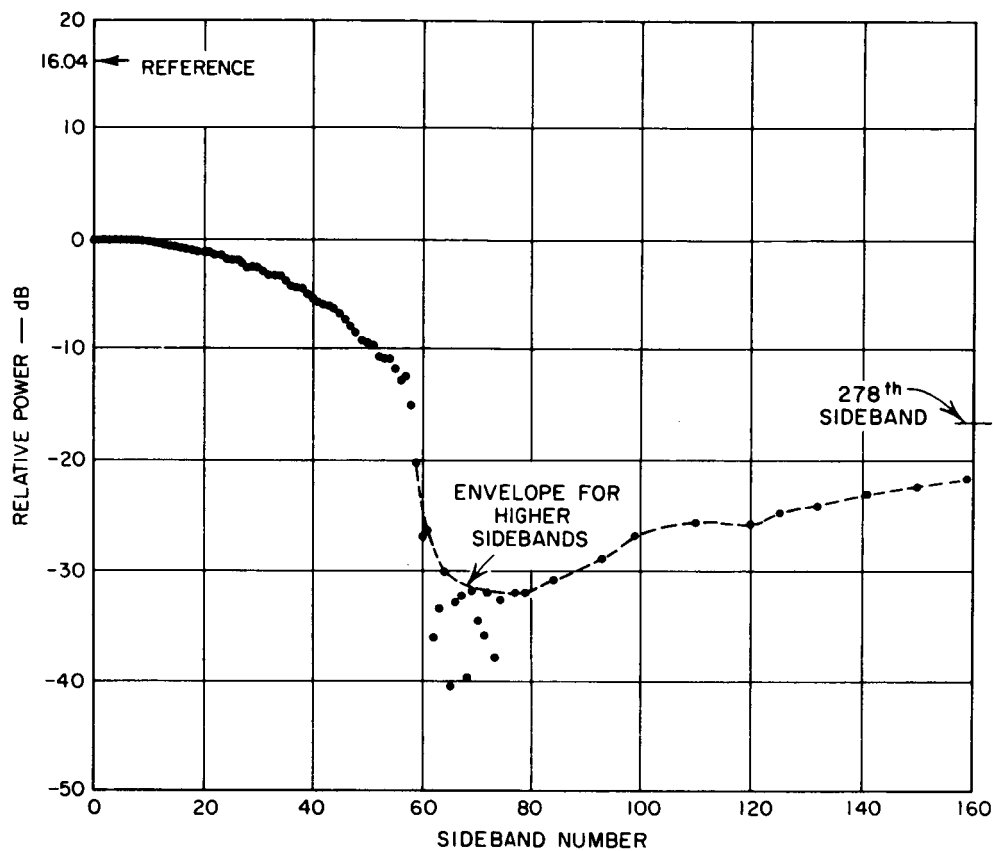
TB-5574-62

FIG. 6 RAY 0 — RELATIVE POWER IN dB FOR EACH SPECTRAL LINE



TS-5574-63

FIG. 7 RAYS -1, +1 — RELATIVE POWER IN dB FOR EACH SPECTRAL LINE



TB-5574-64

FIG. 8 RAYS -1, 0, +1 — RELATIVE POWER IN dB FOR EACH SPECTRAL LINE

compared to the energy in those spectral lines whose numbers are multiples of N . The contribution to the intermediate sidebands of completely inactive elements corresponds to the case where only the inactive elements are operating, except for a reversal of phase.

These considerations can also be applied to the case of an adaptive receiving antenna of the same configuration.

2. Considerations of Total Spectral Power

In Appendix C, the power associated with the infinite number of rays that can exist in a typical Type-1 antenna, having primary dimensions of $R = 10$ (units of wavelength) and $L = 3$, has been calculated. It is shown that the total power, as obtained by summing the spectral content over the first 200 sidebands, associated with Ray 0, is 90% of a theoretical total and that associated with Rays -1 and +1 an additional 9%. Consequently,

consideration of only these three rays is quite justified except when extremely detailed knowledge of the spectral content or other characteristics is needed.

When only the first two significant rays are considered, as has previously been done for computing re-radiation patterns,² it can be postulated that only about 2 to 3 percent of the total power was not accounted for. In general this small amount of power would only produce minor modifications to the sidelobe structure, since it would never tend to form a plane wavefront.

3. The Retrodirective-Array Case

In this portion of the study the antenna as a whole was considered when operating in the retrodirective (receive, transmit) mode with generally different receive (pilot) and transmit frequencies. Only an unmodulated pilot and retransmitted signal were treated and these differed by up to 10% of the carrier frequency. Both the relative gain in the retrodirection as a function of rotation and the spectrum of the transmitted signal were obtained. The mathematical analysis is given in Appendix D. Separate linear amplifiers and ideal mixers behind the elements were assumed, except that in a second computation of spectral content saturated (sometimes called hard limited) amplifiers were assumed.

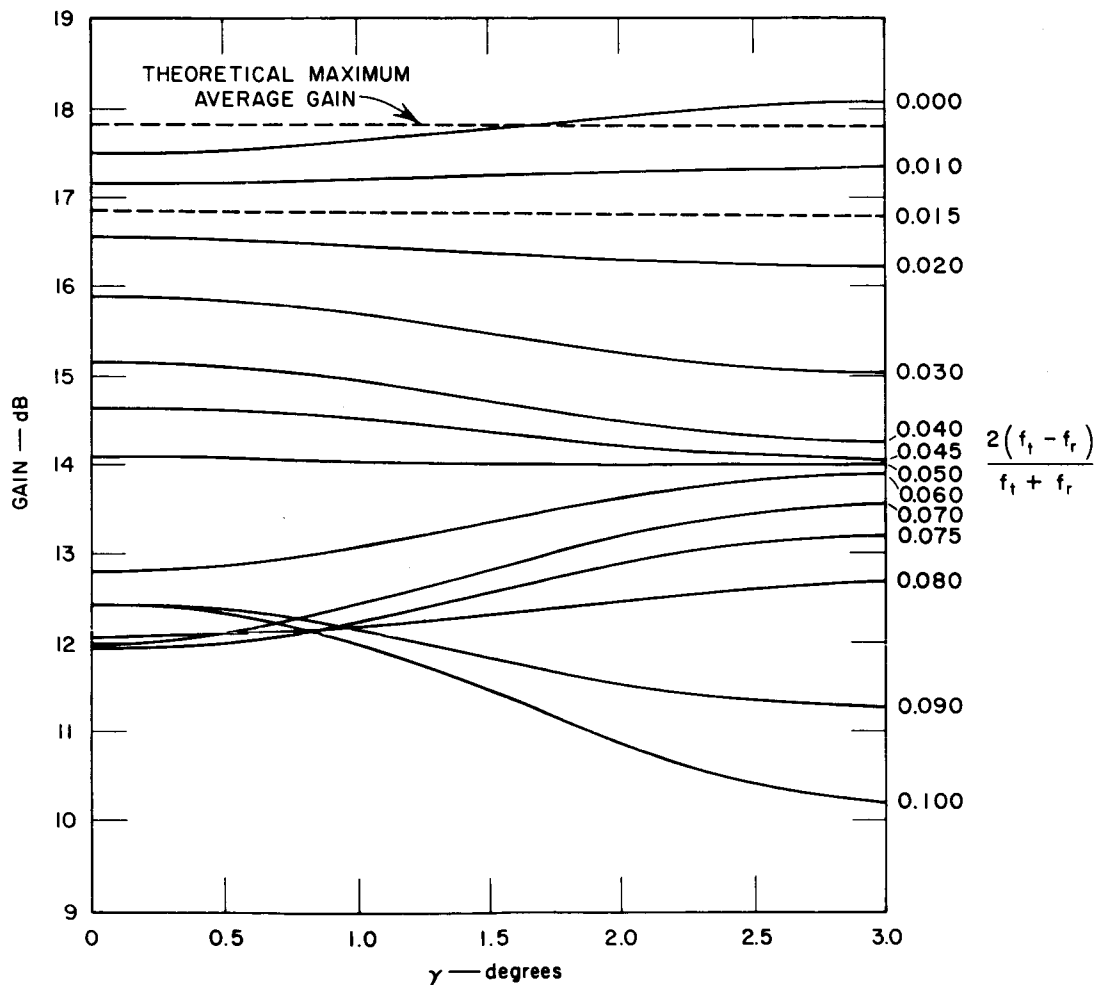
a. Gain in the Retrodirective Direction

This computation of gain as a function of azimuthal angle is similar to one previously performed² except that different receive and transmit frequencies were used, and the gain was computed for many azimuthal positions of the antenna. This computation is not directly related to spectral splitting since the gain is computed for steady-state azimuthal positions of the antenna. However, if the gain varies for different positions, there will obviously be some spectral splitting, due to amplitude modulation at least, as the antenna rotates. The computations show that in the special case of the receive and transmit frequencies being exactly equal, the spectral splitting is due entirely to this amplitude modulation.

Equation (D-11) was evaluated assuming that all elemental radiators were active, for a variety of receive and transmit frequencies f_t and f_r . In all cases the lens mean radius R corresponds to 10 average

wavelengths and the lens length to 3 radii. Since 60 elements were assumed, a range of only 0 to 3 degrees, representing half a period, needs to be considered. Some of the results are shown in Fig. 9. (Other data are shown in Table I, presented later.) The quantity plotted is the ratio of the actual power in the retrodirective beam to the power that would have been transmitted by a single omnidirectional element of equal gain in the axial plane. As has been discussed elsewhere,^{1,2,3,4} the maximum anticipated gain, averaged over all azimuthal directions, is given by

$$10 \log_{10} N = 17.78 \text{ dB for } N = 60 .$$



TC-5574-65

FIG. 9 RETRODIRECTIVE GAIN AS A FUNCTION OF AZIMUTHAL POSITION

As can be seen in Fig. 9, this maximum gain, when averaged over a complete period, is very nearly realized (within 0.02 dB) when $f_t = f_r$. The gain in the direction exactly between two elements ($\gamma = 3$ degrees) has the maximum value and is a fraction of a dB higher than the gain in the direction through an element. This will lead to amplitude modulation as the antenna rotates, but if R and/or L were varied from their present values it would be reasonable to postulate that a set of values could be found in which the gain variation with rotation was very small. Under these conditions (and again with $f_t = f_r$ and all elements identical except for phase) there would theoretically be no spectral splitting. It can also be seen from Fig. 9 that when $f_t \simeq 1.015 f_r$ there is virtually no variation in gain. However, this does not mean that there will be no spectral splitting, as can be seen in Sec. II-B-3-b, below. The reason for this is that while there is no amplitude modulation, there is phase modulation, something which is not present when $f_t = f_r$.

While a rotating antenna structure will generally give rise to spectral splitting, the retransmitted carrier is definitely related to the characteristics of the antenna and the spin rate and, if the pilot signal is unmodulated, will have a symmetrical line spectrum centered on the carrier with nearly all the power in the carrier. Apart from the carrier only the N th sideband (of the spin frequency) has been shown to have appreciable power content (see Sec. II-B-3-b).

While such a signal received at the ground station is moderately complex, it can be synthesized at the final receiver to allow synchronous detection. The synthesis could be done on a computer and would, of course, use the design characteristics of the spacecraft, and consequently have only to track the spin rate of the satellite. The sidebands other than the N th could be ignored, probably resulting in some small amount of distortion. However, except when several elemental radiators were inactive or otherwise faulty such distortion should be minimal.

On the other hand, non-synchronous energy detection is easily implemented if the modulation is frequency-shift keyed (FSK) and the separation of the two frequencies is made somewhat larger than the spectrum spreading due to the combination of communication bit rate and rotation of the antenna.

Considerations of suitable modulation methods do not form part of this study.

b. Spectral-Power Content

In addition to the above computations of gain variation, a study was made of the actual relative power in each of the spectral lines associated with the same antenna operating at the same range of frequencies. In this case, however, not only was the case of linear amplifiers for each elemental phase-conjugating circuit considered, but also the more practical case of equal-output-power (*i.e.*, saturated) amplifiers for each element.

A computer program was developed to calculate this power spectrum for the retrodirected wave from the same cylindrical, geodesic-lens, biconical-horn antenna with 60 elemental radiators, a length equal to 3 radii, and a radius equal to 10 wavelengths at the average carrier frequency. The received frequency lay below the average carrier frequency and the transmitted frequency above it by equal amounts. Three rays were considered for both reception and transmission. Since the elements were considered to be identical, only spectral lines corresponding to the cogging frequency were present (the cogging frequency is equal to the number of elemental radiators times the spin rate of the antenna).

Both linear and saturated (hard-limited) amplifiers were considered. The results for the first and second sidebands of the cogging frequency are presented in Table I. All higher harmonics lie well below those tabulated for the linear-amplifier case. With saturated amplifiers, the powers of all higher harmonics lie below the first harmonic but some are slightly larger than the second harmonic.

These harmonics are due to both amplitude and phase modulation. The component attributable to phase modulation increases with the difference between the received and transmitted frequencies, while that portion attributable to amplitude modulation oscillates.

In all cases the upper and lower sidebands were found to be equal, apparently corresponding to the even property of the retrodirected wave with respect to the instant when the retrodirection passed through an elemental radiator. The powers listed in Table I represent the total power in both the lower and upper sidebands.

In all cases considered, the spectrum spreading due to antenna rotation leaves nearly all the power in the carrier and should have only a minor effect on the operation of the system compared to the expected effects of random noise.

Table I

GAIN AND SIDEBAND POWER FOR A 60-ELEMENT,
CYLINDRICAL-GEODESIC-LENS BICONICAL-HORN
(TYPE-1) ANTENNA IN THE RETRODIRECTIVE MODE

$\frac{2(f_t - f_r)}{f_t + f_r}$	LINEAR AMPLIFIER CASE				SATURATED AMPLIFIER CASE			
	Average Antenna Gain (dB down)*	Sideband Power (dB down)			Average Antenna Gain (dB down)*	Sideband Power (dB down)		
		60th Sidebands, Relative to		120th Sidebands Relative to Carrier		60th Sidebands, Relative to		120th Sidebands Relative to Carrier
		Carrier	Omni-Azimuth			Carrier	Omni-Azimuth	
0.000	0.0177	26.57	8.80	74.77	0.3825	33.97	16.57	127.90
0.005	0.16	26.42	8.80	71.94	0.49	29.76	12.47	57.04
0.010	0.53	26.04	8.79	68.35	0.74	27.22	10.18	52.58
0.015	0.96	25.60	8.78	66.14	1.10	26.55	9.87	55.01
0.020	1.40	25.14	8.76	65.22	1.55	27.65	11.42	59.12
0.025	1.86	24.65	8.73	65.46	2.06	30.77	15.05	54.20
0.030	2.31	24.16	8.69	66.97	2.59	33.54	18.35	49.87
0.035	2.72	23.70	8.64	69.60	3.18	28.87	14.27	48.73
0.040	3.00	23.25	8.46	70.72	3.76	24.72	10.70	52.26
0.045	3.42	22.80	8.44	67.87	4.32	22.91	9.45	62.92
0.050	3.73	22.38	8.33	65.00	4.83	23.07	10.12	52.67
0.055	4.05	21.98	8.25	63.39	5.36	25.24	12.82	58.06
0.060	4.44	21.61	8.27	62.99	5.86	29.70	17.88	53.62
0.065	4.73	21.27	8.22	63.79	6.30	28.51	17.03	57.15
0.070	5.00	20.93	8.16	65.73	6.70	23.15	12.07	56.57
0.075	5.24	20.58	8.04	67.80	7.06	20.15	9.43	50.17
0.080	5.40	20.23	7.85	66.86	7.37	19.20	8.79	45.57
0.085	5.66	19.89	7.77	64.07	7.58	20.07	9.83	41.65
0.090	5.90	19.57	7.69	62.07	7.68	23.35	13.25	40.37
0.095	6.21	19.28	7.71	61.26	7.74	28.87	18.83	46.95
0.100	6.45	--	--	--	7.88	24.13	14.23	47.26

* Relative to the theoretical maximum average antenna gain of 17.78 dB.

Also shown in Table I are the corresponding values of computed antenna gain in the retrodirection, averaged over all azimuthal angles and compared with the theoretical maximum average gain given by $10 \log_{10} 60 = 17.78$ (see also Fig. 9). When linear amplifiers are used it is noticed that the gain decreases monotonically with increasing separation of f_t and f_r , as does the relative power of the 60th sideband when linear amplifiers are used. This gain data has been used to compute approximate values for the 60th sideband power relative to what might be called the omni-azimuthal level—that is, the level that would result if the antenna consisted of just a single omni-directional element located

on the spin axis and having the same gain in the plane of the axis as the complete 60-element antenna. These values are also listed in Table I and are found to be remarkably constant, decreasing by only one dB while the retrodirective gain decreased by over six dB.

When saturated elemental amplifiers are assumed, it can be seen that the computed gain in the retrodirection relative to the carrier power is lower than that for linear amplifiers. This was to be expected since previous work^{2,4} has shown that when the power fed to an element of an antenna array is in proportion to the gain of that element in the desired direction, the gain resulting from all the elements of the array in that direction will be higher than when equal power is fed to the elements. It is also noticed, however, that the sideband power for this model is, in general, considerably less than for the case of linear amplifiers. When the total sideband powers for the first cogging frequency are normalized against the omni-azimuthal power, it can be seen that the values are by no means constant and again are lower than when linear amplifiers are considered; for some values of frequency separations the power is as much as 10 dB lower.

The fact that the sideband power values are not as "well behaved" when saturated amplifiers are used, is compatible with earlier observations made on computed re-radiation patterns² in which it was found that antennas using linear amplifiers had patterns with more regular sidelobe structure than when saturated amplifiers were used.

III ANALYSIS

The analysis, like the rest of this report, will be restricted to considerations of spectral splitting—that is to say, the broadening brought about solely by the rotation of an antenna of what would be a single frequency if the antenna were stationary, into a spectrum of frequencies. Two specific aspects of the problem have been studied and these are discussed separately below. The parameters of the model chosen for investigation gave an element spacing of slightly more than one wavelength. Unfortunately, time did not allow the investigation of elements spaced slightly less than one wavelength apart.

A. Spectral Splitting at a Single Element

It has been shown that if an elemental radiator, which in general would be one of the elements of a circular array, moves in a circular manner it will act as a frequency-modulating device on either a received or transmitted signal. The resultant broadened spectrum is extremely rich in sidebands that are harmonics of the spin frequency. Consideration was given to elements associated with two such arrays, both of which have been the subject of previous investigation during this program period and have been designated Type 3 and Type 1 respectively. It must be stressed that mutual coupling has been neglected in all of the spectral analysis work. Its consideration would greatly complicate the analysis in at least two of the four antenna types considered during this program; these are the Type-2 and Type-3 antennas.

1. Type-3 Antenna

Although the analysis applies strictly only for a single element, consisting of a line-source antenna theoretically having equal gain in all azimuthal directions and arbitrarily high gain in the axial plane, it must be remembered that this element must eventually form part of a complete circular array. Mutual coupling then would be a predominant factor. Since it has been neglected in the present work and since the azimuthal gain function of such an element has been shown to be very far

from constant,⁴ the results of the analysis must be considered purely academic for the present.

The broadened spectrum was shown to consist of a symmetrical spectral band having approximately as many significant lines as the number of correct frequency wavelengths in the locus of two revolutions of the element (*i.e.*, $4\pi R$). The power contained in spectral lines outside this band falls off rapidly although the most significant lines are near the edges of this band. It is anticipated that if mutual coupling were considered, the energy content in lines near the edge of the band would be greatly reduced. This is because the energy content in these lines is associated with the maximum periodic Doppler shift which takes place when the element is at the "limbs" of its circular locus. In practice mutual coupling effects of neighboring elements will in general reduce the azimuthal gain of the subject element when it is at a limb location.

2. Type-1 Antenna

In this analysis it is again assumed that mutual coupling between elements can be neglected, but since it is theoretically possible to reduce this coupling to negligible proportions, by assuring that the lens and aperture portion of the antenna is free of RF reflections, the assumption is quite reasonable. Consequently, analysis of this antenna configuration was carried beyond that for any other type.

Again the spectral content is high over approximately the same band as for a Type-1 antenna of comparable size, but falls off steadily towards the edges of the band. The relative energy content of any particular spectral line is a function of the exact relationship between the wavelength and antenna dimensions. However, it does appear reasonable that the value of N , the number of elemental antennas, can be chosen such that the N th harmonic is small compared with most of the lower-order harmonics. (This is important in a retrodirective antenna, as is indicated in Sec. III-B, below, when only the N th harmonic and its harmonics are important.) This would, however, require that the elements be placed closer together than one wavelength, something which is not difficult to implement, but further analysis would be required to demonstrate that the net effect would indeed be advantageous.

3. Spectral Splitting in an Adaptive Receiving Antenna

The work has not included a study of the case of the self-adaptive receiving antenna system—that is, an array of antenna elements and receiving circuit elements that automatically adjust the phases of all the elements so that their outputs can then be added coherently. However, it is worth mentioning some aspects of spectral splitting as they relate to such a receiving system.

Although it has been shown that in the case of a retrodirective (transmitting) antenna most of the spectral lines cancel each other out on transmission, this is not the case in an adaptive receiving antenna. If phase-locked loops are used in the adaptive circuitry it may not be practical to open up the loop bandwidth sufficiently to allow each voltage-controlled oscillator to follow the incoming pilot signal.

There is some indication that this problem can be easily overcome if the spectral splitting is equivalent to a simple frequency modulation, as is theoretically true for the Type-3 antenna in the academic case where mutual coupling is neglected. No such simple solution has yet been indicated (or sought) for the Type-1 antenna, and the whole subject of the most suitable circuitry to minimize the effects of spectral splitting on antennas of these types warrants further study. It will not, however, be possible to make any such study during the course of the present program.

B. Spectral Splitting and Retrodirective Arrays

The surprising fact demonstrated by the present study is that despite the drastic spectral broadening associated with individual elements of an array, in a properly operating retrodirective array, all but $1/N$ of the spectral lines cancel each other out on transmission in the retrodirection. Even the spectral power associated with the N th harmonic, and its harmonics, is very low and can probably be decreased by appropriate antenna design. It should not present any problem for such simple modulation schemes as power-detected FSK. For instance, if a 60-element, retrodirective, data-modulated antenna is spinning at 10 rpm the information bandwidth received will be broadened by about 20 Hz. If the information bandwidth is comparable, then the broadening might require an appreciable increase in receiver bandwidth and a corresponding decrease in signal sensitivity. However, for information bandwidths of 100 Hz or more, in which energy

detection is used at the ground receiver, the spectrum broadening due to antenna rotation would be insignificant.

If it is desired to use coherent detection, as for instance with phase shift keying (PSK) the problem is more pronounced. In such a case it may be necessary to simulate the spinning antenna at the receiving station. Digital or analogue techniques could be used for such a simulation and could, for instance, take the form of an identical antenna spinning exactly in phase with the distant antenna, allowing of course for the transmission time delay and its derivations (Doppler, etc.). This receiver-based simulator, through which the incoming signal would be processed, could be considered as a device used to "unscramble" the data that has been scrambled in the spinning retrodirective array.

One advantage of such a coherent detection system is that the receiver-based simulator could be modified from time to time to reflect similar changes taking place in the space-vehicle antenna, such as the failure or degradation of one or more of the elemental retransmitters. In addition, if some known asymmetry were introduced into the space vehicle, such as switching off one of the retransmitting elements, then the exact azimuthal orientation of the space vehicle could be obtained at any instant by observing the azimuthal position of the simulating antenna.

The simulating device would have to be calibrated from time to time and this could be done by periodically removing all intentional modulation from the signal and adjusting the simulator or unscrambler, until its output was also unmodulated. Thus a periodic diagnosis of any trouble on the spacecraft could be made, as well as a determination of its orientation. It is obvious that this whole concept requires further study than is presently planned, particularly with regard to noise and appropriate modulation techniques.

A further analysis of the various topics investigated during the course of this program will be included in the First Annual Report on the project.

The stage now seems to have been reached where at least one antenna having a cylindrical configuration shows promise for use on a spin-stabilized vehicle. It therefore seems appropriate that some experimental program should be implemented to demonstrate the feasibility of one or more of the techniques that have so far only been studied theoretically.

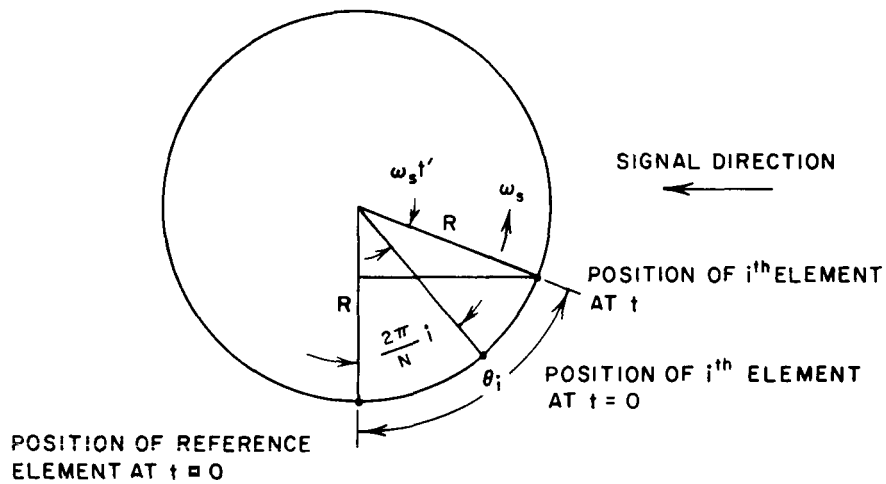
APPENDIX A

**SPECTRAL SPLITTING FOR A SINGLE ELEMENT IN A
CIRCULAR ARRAY OF OMNIDIRECTIONAL ELEMENTS (TYPE-3 ANTENNA)**

APPENDIX A

SPECTRAL SPLITTING FOR A SINGLE ELEMENT IN A
CIRCULAR ARRAY OF OMNIDIRECTIONAL ELEMENTS (TYPE-3 ANTENNA)

Consider a ring of antenna elements on the circumference of a cylinder (see Fig. A-1) spinning at a rate of $\omega_s = 2\pi f_s$ rad/sec. Let a signal be received in the plane containing the ring of elements and hence perpendicular to the spin axis of the satellite. The geometry is shown in Fig. A-1. Mutual coupling is assumed to be negligible so that the radiation pattern of each elemental antenna can be assumed to be omnidirectional (an assumption that is far from true in practice).



TA-5574-66

FIG. A-1 GEOMETRY OF PHASE CENTERS OF ELEMENTAL OMNIDIRECTIONAL RADIATORS

We take the phase at the center of the cylinder as reference and hence write the voltage at that point as

$$v = \cos \omega_0 t$$

where

$$\omega_0 = 2\pi f_0$$

and f_0 is the received frequency which may include a Doppler shift. Such a shift, since it applies equally to all antenna elements, will be called gross Doppler.

Let θ_i be the angle of the i th element with respect to the reference condition. Then,

$$\theta_i = 2\pi \frac{i}{N} + \omega_s t$$

where N is the total number of equally spaced elements. The horizontal displacement from reference is given by

$$\text{disp} = R \sin \theta_i$$

where R is the radius of the circle on which the phase centers of the elemental omnidirectional antennas lie. If we measure this radius in wavelengths and convert to phase in radians, then the signal received by the i th element is

$$\begin{aligned} v_i &= \cos \left[\omega_0 t + 2\pi R \sin \left(\frac{2\pi i}{N} + \omega_s t \right) \right] \\ &= \cos \omega_0 t \cos \left[2\pi R \sin \left(\frac{2\pi i}{N} + \omega_s t \right) \right] \\ &\quad - \sin \omega_0 t \sin \left[2\pi R \sin \left(\frac{2\pi i}{N} + \omega_s t \right) \right] \end{aligned} \quad (\text{A-1})$$

But from Bessel function theory we have

$$\cos (A \sin \theta) = J_0(A) + 2 \sum_{n=1}^{\infty} J_{2n}(A) \cos 2n\theta \quad (\text{A-2a})$$

$$\sin (A \sin \theta) = 2 \sum_{n=0}^{\infty} J_{2n+1}(A) \sin (2n+1)\theta \quad (\text{A-2b})$$

Hence, from Eqs. (A-1) and (A-2),

$$\begin{aligned} v_i &= \cos \omega_0 t \left[J_0(2\pi R) + 2 \sum_{n=1}^{\infty} J_{2n}(2\pi R) \cos 2n \frac{2\pi i}{N} + \omega_s t \right] \\ &\quad - \sin \omega_0 t \left[2 \sum_{n=0}^{\infty} J_{2n+1}(2\pi R) \sin (2n+1) \frac{2\pi i}{N} + \omega_s t \right] \end{aligned} \quad (\text{A-3})$$

But note that

$$\cos \alpha \cos \beta = \frac{1}{2} [\cos (\alpha + \beta) + \cos (\alpha - \beta)] \quad (\text{A-4a})$$

and

$$\sin \alpha \sin \beta = \frac{1}{2} [\cos (\alpha - \beta) - \cos (\alpha + \beta)] \quad (\text{A-4b})$$

and using Eq. (A-4) in (A-3),

$$\begin{aligned} v_i &= J_0(2\pi R) \cos \omega_0 t \\ &+ \sum_{n=1}^{\infty} J_{2n}(2\pi R) \left\{ \cos \left[(\omega_0 + 2n\omega_s) t + \frac{4\pi n i}{N} \right] \right. \\ &+ \left. \cos \left[(\omega_0 - 2n\omega_s) t - \frac{4\pi n i}{N} \right] \right\} \\ &+ \sum_{n=0}^{\infty} J_{2n+1}(2\pi R) \left(\cos \left\{ [\omega_0 + (2n+1)\omega_s] t + \frac{2\pi(2n+1)i}{N} \right\} \right. \\ &\left. - \cos \left\{ [\omega_0 - (2n+1)\omega_s] t - \frac{2\pi(2n+1)i}{N} \right\} \right) \quad (\text{A-5}) \end{aligned}$$

Thus, for the case of ω_0 constant, the voltage at the frequency $(1/2\pi)[\omega_0 + k\omega_s]$ has a magnitude $J_k(2\pi R)$ and a phase $k(2\pi i/N)$.

Note that the phase for $k' = k + \beta N$ for all integers β is the same as for k .

Since it is desirable to maximize the carrier voltage, the antenna radius should be chosen to maximize $J_0(2\pi R)$. If R is near 10 wavelengths, then

$$J_0(2\pi R) \sim \sqrt{\frac{2}{\pi(2\pi R)}} \cos \left(2\pi R - \frac{\pi}{4} \right) \quad (\text{A-6})$$

which has a peak when

$$2\pi R - \frac{\pi}{4} = k(2\pi) \quad (\text{A-7a})$$

or

$$2\pi \left(R - \frac{1}{8} \right) = k2\pi \quad (\text{A-7b})$$

or

$$R = k + \frac{1}{8} \quad . \quad (A-7c)$$

For example, we could take

$$R = 10.125 \quad .$$

When $X > n^2$,

$$J_n(X) \sim \sqrt{\frac{2}{\pi(X)}} \cos \left(X - \frac{n\pi}{2} - \frac{\pi}{4} \right) \quad .$$

The choice of $X = 2\pi[k + (1/8)]$ will make $[X - (n\pi/2) - (\pi/4)] \bmod 2\pi = (\pi/2)n$ and hence the lower odd sidebands will vanish.

The spectrum resulting from this particular model is given in Table A-1.

Table A-1*

SPECTRAL CONTENT vs. SIDEBAND NUMBER

n	$J_n(63.61)$	$ J_n(63.61) ^2$	RELATIVE dB
0	.10003	.010006	0.0
1	-.00013	.000000	$-\infty$
2	-.10003	.010006	0.0
3	-.00615	.000038	-24.2
4	.09945	.009890	0.0
5	.01866	.000348	-14.6
6	-.09652	.009316	-0.3
7	-.03687	.001359	-8.7
8	.08840	.007815	-1.1
9	.05911	.003494	-4.6
10	-.07168	.005138	-2.9
11	-.08146	.006636	-1.8
12	.04344	.001887	-7.3
13	.09804	.009612	-0.2
14	-.00337	.000011	-29.8
15	-.09952	.009904	0.0
16	-.04356	.001897	-7.2
17	.07760	.006022	-2.2
18	.08504	.007232	-1.4
19	-.02947	.000868	-10.6
20	-.10265	.010537	0.2
21	-.03507	.001230	-9.1
22	.07949	.006319	-2.0
23	.09006	.008111	-0.9
24	-.01436	.000206	-17.0
25	-.10090	.010181	0.1

Table A-1* (Concluded)

n	$J_n(63.61)$	$ J_n(63.61) ^2$	RELATIVE dB
26	-.06495	.004219	- 3.7
27	.04780	.002285	- 6.5
28	.10553	.011137	0.5
29	.04510	.002034	- 7.0
30	-.06440	.004147	- 3.8
31	-.10585	.011204	0.5
32	-.03877	.001503	- 8.2
33	.06685	.004469	- 3.5
34	.10813	.011692	0.7
35	.04874	.002376	- 6.3
36	-.05449	.002969	- 5.3
37	-.11042	.012193	0.9
38	-.07396	.005470	- 2.6
39	.02204	.000486	-13.1
40	.10100	.010201	0.1
41	.10498	.011021	0.4
42	.03432	.001178	- 9.3
43	-.05964	.003557	- 4.5
44	-.11497	.013218	1.2
45	-.09940	.009880	- 0.5
46	-.02567	.000659	-11.8
47	.06227	.003878	- 4.1
48	.11769	.013851	1.4
49	.11535	.013306	1.2
50	.06002	.003602	- 4.4
51	-.02099	.000441	-13.5
52	-.09368	.008776	- 0.6
53	-.13218	.017472	2.4
54	-.12658	.016022	2.0
55	-.08273	.006844	- 1.6
56	-.01649	.000272	-15.7
57	.05369	.002883	- 5.4
58	.11273	.012708	1.0
59	.15187	.023064	3.6
60	.16901	.028564	4.6
61	.16695	.027872	4.5
62	.15120	.022861	3.6
63	.12780	.016333	2.1
64	.10194	.010391	0.2
65	.07733	.005980	- 2.2
66	.05610	.003147	- 5.0
67	.03909	.001528	- 8.2
68	.02625	.000689	-11.6
69	.01703	.000290	-15.4
70	.01070	.000114	-19.5
71	.00652	.000043	-23.7
72	.00385	.000015	-28.2
73	.00220	.000005	-33.1
74	.00120	.000001	-40.0
75	.00059	.000000	- ∞

* Tables of the Bessel Functions of the First Kind, ANNALS III of the Computation Laboratory of Harvard University (Oxford University Press, 1947).

APPENDIX B

**DERIVATION OF SPECTRUM IN THE
CYLINDRICAL-GEODESIC-LENS BICONICAL-HORN
ADAPTIVE (TYPE-1) ANTENNA DUE TO VEHICLE ROTATION**

APPENDIX B

DERIVATION OF SPECTRUM IN THE
CYLINDRICAL-GEODESIC-LENS BICONICAL-HORN
ADAPTIVE (TYPE-1) ANTENNA DUE TO VEHICLE ROTATION

This antenna has been described in the First Quarterly Report, and its general configuration is shown in Fig. 3 in the main text. For the present purpose we note that each elemental radiator, at the instant when its angular position relative to the direction of the received signal is

$$\gamma, \quad -\pi \leq \gamma \leq \pi \quad (\text{B-1})$$

receives signals from an infinite number of directions, α_i , where α_i is measured relative to the direction of maximum gain and

$$-\frac{\pi}{2} < \alpha_i < \frac{\pi}{2} \quad (\text{B-2})$$

(see Fig. 4).

Due to the nature of the lens and the geometry we find

$$\alpha_i + L \tan \alpha_i = 2\pi i + \gamma \quad (\text{B-3})$$

where $i = 0, \pm 1, \pm 2, \pm 3, \pm \dots$, and L is the ratio of the height of the lens to its radius.

It can be shown¹ that each signal can be written as

$$F_i(\gamma) = \frac{G(\alpha_i)}{\left(1 + \frac{L}{\cos^2 \alpha_i}\right)^{1/2}} \exp j \left[\omega_0 t + 2\pi R \left(\frac{L}{\cos \alpha_i} - \cos \alpha_i \right) \right] \quad (\text{B-4})$$

where $G(\alpha)$ is the voltage gain function of the elemental radiator within the "parallel plate" lens region. A typical gain function can be described by:

$$G(\alpha) = 10 \exp - 2.4 \left(\frac{\pi R \alpha}{N} \right)^2 \quad (\text{B-5})$$

where R is the radius in wavelengths, N is the number of elemental radiators, and the phase is measured with respect to a fixed but arbitrary point.

The $[1 + (L/\cos^2 \alpha)]^{-1/2}$ term is due to space taper in the lens. ω_0 is, of course, the RF angular frequency including gross Doppler.

If the antenna is rotating (spin-stabilized), then the angle γ is a periodic sawtooth function of time; hence both the amplitude and relative phase of $F_i(\gamma)$ are also periodic and have a fundamental frequency proportional to the spin rate.

Let ω_s be the angular velocity of the antenna in radians per second. Then γ is periodic and can be written

$$\gamma = \omega_s t \text{ for } |t| \leq \frac{\pi}{\omega_s} \quad (\text{B-6})$$

Thus the signals, from Eqs. (B-4) and (B-6), can be written as

$$F_i(t) = \frac{G(\alpha_i)}{H(\alpha_i)} \exp j[\omega_0 t + \varphi(\alpha_i)] \quad (\text{B-7})$$

where

$$H(\alpha_i) = \left[1 + \frac{L}{\cos^2 \alpha_i} \right]^{1/2} \quad (\text{B-8})$$

and

$$\varphi(\alpha_i) = 2\pi R \left[\frac{L}{\cos \alpha_i} - \cos \alpha_i \right] \quad (\text{B-9})$$

Of course, since

$$\alpha_i + L \tan \alpha_i = 2\pi i + \omega_s t \quad (\text{B-10})$$

α_i is a function of t and is also periodic. Since $F_i(t)$ is periodic, we can write it in terms of a carrier and sidebands as

$$F_i(t) = \sum_{k=-\infty}^{\infty} C_{ik} e^{j(\omega_0 t + k\omega_s t + \varphi_{ik})} \quad (\text{B-11})$$

Now, equate Eqs. (B-7) and (B-11) and cancel $e^{j\omega_0 t}$, getting:

$$\sum_{k=-\infty}^{\infty} (C_{ik} e^{j\varphi_{ik}}) e^{jk\omega_s t} = \frac{G(\alpha_i)}{H(\alpha_i)} e^{j\varphi(\alpha_i)} \quad (B-12)$$

Multiply both sides by $e^{-jk\omega_s t}$ and integrate over a period:

$$C_{ik} e^{j\varphi_{ik}} = \frac{1}{T} \int_{-T/2}^{T/2} \frac{G(\alpha_i)}{H(\alpha_i)} e^{j[\varphi(\alpha_i) - k\omega_s t]} dt \quad (B-13)$$

Now, transform the integration from t to α according to Eq. (B-10) and note that

$$\omega_s = 2\pi f_s = \frac{2\pi}{T} \quad (B-14)$$

Now,

$$d\alpha_i \left(1 + \frac{L}{\cos^2 \alpha_i} \right) = \omega_s dt \quad (B-15)$$

and when $t = -(T/2)$,

$$\alpha_i + L \tan \alpha_i = 2\pi i - \pi = (2i - 1)\pi \quad (B-16)$$

Let the solution of Eq. (B-16) be B_i . Similarly, when $t = +(T/2)$,

$$\alpha_i + L \tan \alpha_i = 2\pi i + \pi = (2i + 1)\pi \quad (B-17)$$

and let the solution be C_i . Thus we are numbering the rays as $i = 0, \pm 1, \pm 2, \pm 3$ etc., and we have

$$B_i + L \tan B_i = (2i - 1)\pi \quad (B-18a)$$

$$C_i + L \tan C_i = (2i + 1)\pi \quad (B-18b)$$

Using these results in Eq. (B-13), we obtain

$$C_{ik} e^{j\varphi_{ik}} = \frac{1}{2\pi} \int_{B_i}^{C_i} G(\alpha_i) H(\alpha_i) e^{j(\varphi(\alpha_i) - k(\alpha_i + L \tan \alpha_i + 2\pi i))} d\alpha_i \quad (B-19)$$

Since $e^{-j(k2\pi i)} = 1$, it can be omitted.

Now consider the summed effect over all rays:

$$\begin{aligned}
C_k e^{j\varphi_k} &= \sum_{i=-\infty}^{+\infty} C_{ik} e^{j\varphi_{ik}} \\
&= \frac{1}{2\pi} \sum_{i=-\infty}^{\infty} \int_{B_i}^{C_i} G(\alpha) H(\alpha) e^{j[\varphi(\alpha) - k(\alpha + L \tan \alpha)]} d\alpha \quad . \quad (B-20)
\end{aligned}$$

These are non-overlapping adjacent ranges of integration. From the monotonic functions of Eq. (B-18):

$$\begin{aligned}
C_0 &\sim \pi, & B_1 &\sim \pi \\
C_1 &\sim 3\pi, & B_2 &\sim 3\pi \\
B_0 &\sim -\pi, & C_{-1} &\sim -\pi \\
B_{-1} &\sim -3\pi, & C_{-2} &\sim -3\pi \quad .
\end{aligned}$$

Further,

$$\lim_{i \rightarrow \infty} B_i = \lim_{i \rightarrow \infty} C_i = \pi/2$$

and

$$\lim_{i \rightarrow -\infty} B_i = \lim_{i \rightarrow -\infty} C_i = -\pi/2 \quad .$$

Thus, Eq. (B-20) becomes

$$C_k e^{j\varphi_k} = \frac{1}{2\pi} \int_{-\pi/2}^{\pi/2} G(\alpha) H(\alpha) e^{j[\varphi(\alpha) - k(\alpha + L \tan \alpha)]} d\alpha \quad . \quad (B-21)$$

Now use Euler's equation, $e^{j\varphi} = \cos \varphi + j \sin \varphi$, to write

$$C_k \cos \varphi_k = \frac{1}{2\pi} \int_{-\pi/2}^{\pi/2} G(\alpha) H(\alpha) [\cos \varphi(\alpha) \cos k\delta - \sin \varphi(\alpha) \sin k\delta] d\alpha \quad (B-22)$$

where

$$\delta = \alpha + L \tan \alpha \quad . \quad (B-23)$$

From Eqs. (B-5), (B-8), and (B-9) we note that $G(\alpha)$, $H(\alpha)$, and $\varphi(\alpha)$ are all even functions of α . $\cos k\delta$ is also even in α , but $\sin k\delta$ is odd.

Since the integral of an even function over a range symmetrical about the origin is twice the integral over the half-range and the integral of an odd function is zero, we have

$$C_k \cos \varphi_k = \frac{1}{\pi} \int_0^{\pi/2} G(\alpha)H(\alpha) \cos \varphi(\alpha) \cos k(\alpha + L \tan \alpha) d\alpha \quad . \quad (\text{B-24})$$

Similarly,

$$\begin{aligned} C_k \sin \varphi_k &= \frac{1}{2\pi} \int_{-\pi/2}^{\pi/2} G(\alpha)H(\alpha) [\sin \varphi(\alpha) \cos k\delta - \cos \varphi(\alpha) \sin k\delta] d\alpha \\ &= \frac{1}{\pi} \int_0^{\pi/2} G(\alpha)H(\alpha) \sin \varphi(\alpha) \cos k(\alpha + L \tan \alpha) d\alpha \quad . \quad (\text{B-25}) \end{aligned}$$

Note further that Eqs. (B-24) and (B-25) are even functions of k so that

$$C_{-k} \cos \varphi_{-k} = C_k \cos \varphi_k \quad (\text{B-26a})$$

and

$$C_{-k} \sin \varphi_{-k} = C_k \sin \varphi_k \quad . \quad (\text{B-26b})$$

Thus the spectrum is symmetrical about the carrier.

Equations (B-24) and (B-25), by a change in the upper limit of integration, can also be used to find the spectrum of Ray 0 and the spectrum for Rays -1, 0, and 1. By changing both limits of integration, the spectrum for Rays -1 and 1 can also be found.

An Algol program for the Burroughs 5500 has been prepared and run to obtain spectrum data, using $R = 10$, $L = 3$, $N = 60$, for the following ray groupings:

Ray 0
Rays -1 and +1
Rays -1, 0, and +1 .

The following was computed for each sideband:

Inphase component	$C_k \cos \varphi_k$
Quadrature components	$C_k \sin \varphi_k$

Amplitude	C_k
Phase angle	φ_k
Power relative to carrier	P_{dB}
Cumulative power	$\sum_{i=0}^k P_k$

APPENDIX C

DERIVATION OF POWER IN THE TYPE-1 ANTENNA

APPENDIX C

DERIVATION OF POWER IN THE TYPE-1 ANTENNA

Since a lossless system has been assumed, it is of interest to calculate the power emitted from an elemental radiator in each ray.

The voltage gain function of each elemental radiator as measured in the "parallel plate" region of the lens is assumed given by:

$$G(\alpha) = 10^{[-2.4(\pi R\alpha/N)^2]} \quad (C-1)$$

Hence the power gain is

$$G^2(\alpha) = 10^{[-4.8(\pi R\alpha/N)^2]} \quad (C-2a)$$

$$= e^{-(K^2\alpha^2/2)} \quad (C-2b)$$

Hence

$$\ln G^2(\alpha) = -\frac{K^2\alpha^2}{2} = -48\left(\frac{\pi R\alpha}{N}\right)^2 \ln 10$$

or

$$K = \frac{\pi R}{N} (4.701). \quad (C-3)$$

Then the power can be written

$$P_0 = \int_0^{\alpha_0} G^2(\alpha) d\alpha \quad \text{for Ray 0} \quad (C-4a)$$

$$= 2 \int_0^{\pi/2} G^2(\alpha) d\alpha \quad \text{for all rays} \quad (C-4b)$$

$$= 2 \int_{\alpha_0}^{\alpha_1} G^2(\alpha) d\alpha \quad \text{for Rays -1 and +1} \quad (C-4c)$$

$$= 2 \int_0^{\alpha_1} G^2(\alpha) d\alpha \quad \text{for Rays -1, 0, and +1} \quad (C-4d)$$

where $\alpha_0 = 0.687$ radians, and satisfies

$$\alpha_0 + L \tan \alpha_0 = \pi \text{ for } L = 3 \quad (\text{C-5})$$

and $\alpha_1 = 1.226$ radians, and satisfies

$$\alpha_1 + L \tan \alpha_1 = 3\pi \text{ for } L = 3 \quad (\text{C-6})$$

But in all cases

$$\begin{aligned} P &= 2 \int_0^{\hat{\alpha}} G^2(\alpha) d\alpha \\ &= 2 \int_0^{\hat{\alpha}} e^{-(K^2 \alpha^2 / 2)} d\alpha \end{aligned} \quad (\text{C-7})$$

and setting $x = K\alpha$, $dx = Kd\alpha$,

$$\begin{aligned} P &= \frac{2}{K} \int_0^{K\hat{\alpha}} \frac{e^{-(x^2/2)}}{\sqrt{2\pi}} dx \\ &= \frac{2\sqrt{2\pi}}{K} \left(\frac{1}{\sqrt{2\pi}} \int_0^{K\hat{\alpha}} e^{-(x^2/2)} dx \right) \end{aligned} \quad (\text{C-8})$$

where the expression in parentheses can be found in the tables of the normal probability density.

When Eq. (C-8) is evaluated for $R = 10$ and $N = 60$ and compared with the cumulative power from the computer runs, we find:

Rays	Eq. (C-8)	Computer (200 sidebands)
All	1.020	--
0	0.926	0.918
-1,1	0.089	0.098
-1,0,1	1.014	1.008

These results show sufficient agreement to verify the computer algorithm used.

The relative power in Rays -1, 0, and +1 as compared with the total power from an elemental radiator (1.014/1.020) certainly indicates that the higher-ordered rays should have a negligible effect on the overall spectrum of the signals.

APPENDIX D

**RETRANSMITTED SIGNAL FROM A CYLINDRICAL-GEODESIC-LENS
BICONICAL-HORN ADAPTIVE (TYPE-1) ANTENNA**

APPENDIX D

RETRANSMITTED SIGNAL FROM A CYLINDRICAL-GEODESIC-LENS BICONICAL-HORN ADAPTIVE (TYPE-1) ANTENNA

1. Introduction

As discussed earlier in this report, almost all the power is contained in Rays $-1, 0, 1$ and therefore the present discussion will be restricted to these rays. It is assumed that each elemental antenna of the array is connected to a simple conjugating circuit.

Power is received at each elemental radiator along each of the three ray paths. The corresponding voltages are added and mixed with a pure sinewave at twice pilot frequency. The difference signal from the mixer is then retransmitted along each of the three ray paths.

To begin with, let us assume the following:

- (1) The local oscillator is at exactly twice the incoming pilot frequency.
- (2) All operations are linear.
- (3) Phase delays are negligible compared to spin period.

Each signal in passing from the plane external wave to the elemental radiator in either direction has its amplitude reduced by $G(\alpha)/H(\alpha)$ and undergoes a phase delay of $2\pi R[(L/\cos \alpha) - \cos \alpha]$ where

$$G(\alpha) = e^{-(\kappa^2 \alpha^2 / 2)} \quad (D-1)$$

$$H(\alpha) = \left(1 + \frac{L}{\cos^2 \alpha}\right)^{1/2} \quad (D-2)$$

R = Radius in wavelengths

L = Length in radii

and

$$\alpha_{-1} + L \tan \alpha_{-1} = -2\pi + \gamma \quad (\text{D-3a})$$

$$\alpha_0 + L \tan \alpha_0 = \gamma \quad (\text{D-3b})$$

$$\alpha_1 + L \tan \alpha_1 = 2\pi + \gamma \quad (\text{D-3c})$$

where γ is the angle of arrival with respect to the position of the elemental radiator.

For convenience, let

$$\varphi_i = 2\pi R \left(\frac{L}{\cos \alpha_i} - \cos \alpha_i \right) \quad (\text{D-4})$$

$$A_i = \frac{G(\alpha_i)}{H(\alpha_i)} \quad (\text{D-5})$$

Note that the effect of the mixer is to change the sign of the phase.

2. Derivation

The voltage reaching the elemental radiator (assuming unit voltage in the arriving wave) is

$$A_{-1} \angle \varphi_{-1} + A_0 \angle \varphi_0 + A_1 \angle \varphi_1 \quad (\text{D-6})$$

After mixing, we have

$$A_{-1} \angle -\varphi_{-1} + A_0 \angle -\varphi_0 + A_1 \angle -\varphi_1 \quad (\text{D-7})$$

Then the total retransmitted signal in the direction γ consists of nine terms:

$$\begin{aligned} V = & A_{-1}^2 \angle 0 + A_{-1} A_0 \angle (\varphi_0 - \varphi_{-1}) + A_{-1} A_1 \angle (\varphi_1 - \varphi_{-1}) \\ & + A_0 A_{-1} \angle (\varphi_{-1} - \varphi_0) + A_0^2 \angle 0 + A_0 A_1 \angle (\varphi_1 - \varphi_0) \\ & + A_1 A_{-1} \angle (\varphi_{-1} - \varphi_1) + A_1 A_0 \angle (\varphi_0 - \varphi_1) + A_1^2 \angle 0 \quad (\text{D-8}) \end{aligned}$$

Rearranging Eq. (D-8) and combining terms having equal positive and negative angles gives:

$$V = (A_{-1}^2 + A_0^2 + A_1^2)\angle 0 + 2A_{-1}A_0 \cos(\varphi_0 - \varphi_{-1})\angle 0 \\ + 2A_{-1}A_1 \cos(\varphi_1 - \varphi_{-1})\angle 0 + 2A_0A_1 \cos(\varphi_1 - \varphi_0)\angle 0 \quad . \quad (D-9)$$

Equation (D-9) indicates that all components of the retransmitted signal are in phase, but the amplitude of the signal varies with γ and hence with time.

3. Effect of Different Receiving and Transmitting Frequencies

If Assumption 1 is dropped, then R , which is measured in wavelengths, will be different for reception and transmission. L is unchanged.

R enters in the K of Eq. (D-1) and in the phase term. Let R , $G(\alpha)$, A , and φ refer to the received frequency, f_R , and \hat{R} , $\hat{G}(\alpha)$, \hat{A} , and $\hat{\varphi}$ refer to the transmitted frequency f_T .

Then,

$$\frac{\hat{R}}{R} = \frac{f_T}{f_R} R = CR \quad (D-10a)$$

$$\hat{K} = CK \quad (D-10b)$$

$$\hat{\varphi} = C\varphi \quad (D-10c)$$

Note that Eq. (D-3) does not involve R and therefore the $\gamma - \alpha$ relationships are the same for both transmission and reception. Equation (D-7) is still valid, but the equivalent of Eq. (D-8) is

$$\hat{V} = \hat{A}_{-1}\hat{A}_{-1}\angle(\hat{\varphi}_{-1} - \varphi_{-1}) + \hat{A}_{-1}\hat{A}_0\angle(\hat{\varphi}_0 - \varphi_{-1}) \\ + \hat{A}_{-1}\hat{A}_1\angle(\hat{\varphi}_1 - \varphi_{-1}) + \hat{A}_0\hat{A}_{-1}\angle(\hat{\varphi}_{-1} - \varphi_0) \\ + \hat{A}_0\hat{A}_0\angle(\hat{\varphi}_0 - \varphi_0) + \hat{A}_0\hat{A}_1\angle(\hat{\varphi}_1 - \varphi_0) \\ + \hat{A}_1\hat{A}_{-1}\angle(\hat{\varphi}_{-1} - \varphi_1) + \hat{A}_1\hat{A}_0\angle(\hat{\varphi}_0 - \varphi_1) \\ + \hat{A}_1\hat{A}_1\angle(\hat{\varphi}_1 - \varphi_1) \quad . \quad (D-11)$$

Unlike the previous case, Eq. (D-11) indicates that both amplitude and angle modulation will be present.

REFERENCES

1. C. A. Hacking *et al.*, "Study and Applications of Retrodirective and Self-Adaptive Electromagnetic Wave Controls to a Mars Probe," Second Quarterly Report, SRI Project 5574, Contract NAS 2-2933, Stanford Research Institute, Menlo Park, California (February 1966).
2. C. A. Hacking and J. A. Martin, "Study and Application of Retrodirective and Self-Adaptive Electromagnetic Wave Controls to a Mars Probe," First Quarterly Report, Contract NAS 2-2933, SRI Project 5574, Stanford Research Institute, Menlo Park, California (November 1965).
3. C. C. Cutler, R. Kompfner, and L. C. Tillotson, "A Self Steering Array Repeater, " *Bell System Tech. J.*, Vol. 43, No. 5, pp. 2013-2032 (September 1963).
4. A. T. Villeneuve, "Optimization of Gain of Arbitrary Array Antennas," Scientific Report No. 5, Contract AF 19(628)-4349, Hughes Aircraft Co., Culver City, California, Report No. P65-153, HAC Ref. No. A5034 (December 1965).

Security Classification

DOCUMENT CONTROL DATA - R&D

(Security classification of title, body of abstract and indexing annotation must be entered when the overall report is classified)

1. ORIGINATING ACTIVITY (Corporate author) Stanford Research Institute Menlo Park, California		2a. REPORT SECURITY CLASSIFICATION UNCLASSIFIED	
		2b. GROUP	
3. REPORT TITLE STUDY AND APPLICATIONS OF RETRODIRECTIVE AND SELF-ADAPTIVE ELECTROMAGNETIC WAVE CONTROLS TO A MARS PROBE			
4. DESCRIPTIVE NOTES (Type of report and inclusive dates) Third Quarterly Report — Covering the period 1 January to 31 July 1966			
5. AUTHOR(S) (Last name, first name, initial) Hacking, Colin A.; Dawson, Charles H.			
6. REPORT DATE November 1966	7a. TOTAL NO. OF PAGES 52	7b. NO. OF REFS 4	
8a. CONTRACT OR GRANT NO. Contract NAS 2-2933	9a. ORIGINATOR'S REPORT NUMBER(S) Third Quarterly Report SRI Project 5574		
b. PROJECT NO.	9b. OTHER REPORT NO(S) (Any other numbers that may be assigned this report)		
c.			
d.			
10. AVAILABILITY/LIMITATION NOTICES			
11. SUPPLEMENTARY NOTES		12. SPONSORING MILITARY ACTIVITY National Aeronautics and Space Administration Technical Information Division Ames Research Center, Moffett Field, California.	
13. ABSTRACT This report primarily concerns the effects on the spectrum of a received or transmitted CW signal associated with one or the other of two antennas each having a generally cylindrical configuration and spinning about its axis. The spectrum associated with a single element on such an antenna is very broad, with high energy content in high-order sidebands. However, the effect of spinning, on the retransmitted spectrum, of a complete retrodirective antenna is shown to be quite small.			

14. KEY WORDS	LINK A		LINK B		LINK C	
	ROLE	WT	ROLE	WT	ROLE	WT
Self-adaptive antennas Retrodirective antennas Cylindrical configuration Spectral splitting with spin stabilization						

INSTRUCTIONS

1. ORIGINATING ACTIVITY: Enter the name and address of the contractor, subcontractor, grantee, Department of Defense activity or other organization (*corporate author*) issuing the report.

2a. REPORT SECURITY CLASSIFICATION: Enter the overall security classification of the report. Indicate whether "Restricted Data" is included. Marking is to be in accordance with appropriate security regulations.

2b. GROUP: Automatic downgrading is specified in DoD Directive 5200.10 and Armed Forces Industrial Manual. Enter the group number. Also, when applicable, show that optional markings have been used for Group 3 and Group 4 as authorized.

3. REPORT TITLE: Enter the complete report title in all capital letters. Titles in all cases should be unclassified. If a meaningful title cannot be selected without classification, show title classification in all capitals in parenthesis immediately following the title.

4. DESCRIPTIVE NOTES: If appropriate, enter the type of report, e.g., interim, progress, summary, annual, or final. Give the inclusive dates when a specific reporting period is covered.

5. AUTHOR(S): Enter the name(s) of author(s) as shown on or in the report. Enter last name, first name, middle initial. If military, show rank and branch of service. The name of the principal author is an absolute minimum requirement.

6. REPORT DATE: Enter the date of the report as day, month, year; or month, year. If more than one date appears on the report, use date of publication.

7a. TOTAL NUMBER OF PAGES: The total page count should follow normal pagination procedures, i.e., enter the number of pages containing information.

7b. NUMBER OF REFERENCES: Enter the total number of references cited in the report.

8a. CONTRACT OR GRANT NUMBER: If appropriate, enter the applicable number of the contract or grant under which the report was written.

8b, 8c, & 8d. PROJECT NUMBER: Enter the appropriate military department identification, such as project number, subproject number, system numbers, task number, etc.

9a. ORIGINATOR'S REPORT NUMBER(S): Enter the official report number by which the document will be identified and controlled by the originating activity. This number must be unique to this report.

9b. OTHER REPORT NUMBER(S): If the report has been assigned any other report numbers (*either by the originator or by the sponsor*), also enter this number(s).

10. AVAILABILITY/LIMITATION NOTICES: Enter any limitations on further dissemination of the report, other than those

imposed by security classification, using standard statements such as:

- (1) "Qualified requesters may obtain copies of this report from DDC."
- (2) "Foreign announcement and dissemination of this report by DDC is not authorized."
- (3) "U. S. Government agencies may obtain copies of this report directly from DDC. Other qualified DDC users shall request through _____."
- (4) "U. S. military agencies may obtain copies of this report directly from DDC. Other qualified users shall request through _____."
- (5) "All distribution of this report is controlled. Qualified DDC users shall request through _____."

If the report has been furnished to the Office of Technical Services, Department of Commerce, for sale to the public, indicate this fact and enter the price, if known.

11. SUPPLEMENTARY NOTES: Use for additional explanatory notes.

12. SPONSORING MILITARY ACTIVITY: Enter the name of the departmental project office or laboratory sponsoring (*paying for*) the research and development. Include address.

13. ABSTRACT: Enter an abstract giving a brief and factual summary of the document indicative of the report, even though it may also appear elsewhere in the body of the technical report. If additional space is required, a continuation sheet shall be attached.

It is highly desirable that the abstract of classified reports be unclassified. Each paragraph of the abstract shall end with an indication of the military security classification of the information in the paragraph, represented as (TS), (S), (C), or (U).

There is no limitation on the length of the abstract. However, the suggested length is from 150 to 225 words.

14. KEY WORDS: Key words are technically meaningful terms or short phrases that characterize a report and may be used as index entries for cataloging the report. Key words must be selected so that no security classification is required. Identifiers, such as equipment model designation, trade name, military project code name, geographic location, may be used as key words but will be followed by an indication of technical context. The assignment of links, roles, and weights is optional.